Chemistry Africa (2020) 3:1087–1098
https://doi.org/10.1007/s42250-020-00190-z

ORIGINAL ARTICLE

A Green Approach: Evaluation of *Combretum indicum* (CI) Leaf Extract as an Eco-friendly Corrosion Inhibitor for Mild Steel in 1M HCl

Pavithra S. Neriyana[1,2] · Vijaya D . P. Alva[1,2]

Received: 27 July 2020 / Accepted: 30 September 2020 / Published online: 14 October 2020

Abstract
The anticorrosive activity of *Combretum indicum* (CI) leaf extract has been examined on mild steel corrosion in 1M HCl by using weight loss and electrochemical measurement techniques. The results of these experimental techniques have consistent in confirming the effect of the CI leaf extract on corrosion inhibition and a mechanism for the inhibition was proposed. The dissolution rate of steel in acidic solution was found to be sensitive to the concentration of CI leaf extract and the corrosion rate reduces when the concentration of CI leaf extract is increased and reaches the high protection efficiency. The potentiodynamic polarization study confirms the mixed mode of inhibition. Ultraviolet–visible (UV) and Fourier -transform infrared (FTIR) spectroscopic techniques were performed to evaluate the phenomenon of adsorption in the plant extract and the functional groups. The surface morphology analysis (SEM) further corroborates the adsorption of inhibitor molecules over the metal surface.

Keywords Corrosion · Inhibition · Mild steel · CI leaf extract

1 Introduction

Mild steel is one of the most commonly used metal in residential and commercial structures, due to its excellent tensile strength, durability, and low cost. But it has poor resistance to corrosion in acidic environments. Acids are generally used in several industries for the removal of scale and rust. Hydrochloric acid is one of the most aggressive acids which is widely used in industries for pickling processes. Chemically active metals and alloys are affected by the corrosion due to the exposure of metals to the acidic solution. Corrosion is the destruction of a metallic surface due to its interaction with the environment and it can be lowered by using suitable preventive measures. Corrosion inhibition is one of the most practical and convenient techniques to prevent corrosion on metals in an acidic environment. Corrosion inhibitors control the metallic dissolution and acid consumption, by forming a protective layer on the metal surface. A variety of organic compounds were studied as corrosion inhibitors. Literature reveals that organic inhibitors containing heteroatoms such as nitrogen, sulfur, phosphorous, and oxygen with aromatic rings in their structures are excellent inhibitors. But unfortunately, they have high manufacturing costs and toxicity on the environment. Therefore, natural products have been used as environmentally acceptable, readily available, and low-cost inhibitors. Plant extracts are a rich source of natural chemical compounds, which are analogous to organic inhibitors [1–4].

The inhibition effect of various natural products extracted from the plants in an acidic medium for mild steel has been reported by many authors, among that, extracts of *Dardagan* [5], *Rosa canina* [6], *Myrobalan* [7], *Tamarindus indica* [8], *Prosopis farcta* [9], *Glycyrrhiza glabra* [10] and *Ginkgo* [11] were found to be an excellent inhibitors in 1M HCl. The corrosion inhibitive property of *Gentiana olivieri* [12] was observed in 0.5M HCl. *Irvingia wombolu* [13] *Euphorbia heterophylla L* [14] *Cocoa leaf* [15] showed good inhibition efficiency for mild steel in 1.5M HCl. *Tephrosia purpurea* [16] extract prevented the corrosion on the mild steel surface in 1N HCl. Anticorrosive properties of *Aegle marmelos* [17], *Radish leaf* [18], *Armoracia rusticana* [19], and *Artemisia herba-alba oil* [20] were studied in 0.5 M H_2SO_4. *Citrus sinensis (orange)* [21] and *Hardwickia binata roxb* [22]

✉ Vijaya D . P. Alva
alvavijaya@gmail.com

[1] Department of Chemistry, Shree Devi Institute of Technology, Kenjar, Mangalore, Karnataka 574142, India

[2] Affiliated to Visvesvaraya Technological University, Belagavi, Karnataka, India

were investigated as an environmentally friendly corrosion inhibitor in both HCl and H_2SO_4. It is understood that the inhibition efficiency of plant extract is often attributed to the presence of complex constituents of organic species such as tannins, alkaloids, amino acids, carbohydrates, flavonoids, and the presence of heteroatoms, aromatic rings in organic compounds are the major adsorption centers of corrosion inhibitors.

In the present work, *Combretum indicum* (CI) maintains promise for an environmentally friendly corrosion inhibitor. CI is frequently referred to as Ragoon Creeper, which is part of the Combretaceae plant family. This plant can be seen in many areas of India. Parts such as leaves, flowers, and seeds have great medicinal potential. Leaf extract of CI contains numerous phytochemical constituents, such as saponins, alkaloids, flavonoids, tannins, starch, proteins, and glycosides [23]. These natural organic constituents in the leaf extracts have a strong electron-donating capacity with iron and inhibit the corrosion rate of the metal. Herein, the CI leaves were extracted and their inhibition efficiencies were studied for mild steel in 1M HCl. The inhibition performance was discussed using weight loss and electrochemical methods. Scanning Electron Microscope was employed to study the surface morphology and activation parameters were evaluated.

2 Experimental Work

2.1 Material and Electrolyte

Corrosion tests were performed on mild steel samples. Rectangular mild steel specimens of dimension 2.5 cm × 2.5 cm × 0.3 cm were used for gravimetric and cylindrical mild steel rod with an exposed area of 1 cm^2, were used for electrochemical measurements. These samples were mechanically abraded with different grades of emery papers, degreased, rinsed with distilled water, and dried. Fresh CI leaves were collected from the residential region. It was cleaned first with tap water and then with distilled water. The leaves were cut into small pieces and dried in the laboratory under shade for 5 days, and then dried leaves were ground to powder using pestles and mortars. CI leaf extract was prepared by using the Soxhlet method. About 25 g of CI leaf powder was uniformly packed and placed in a thimble. It was extracted with distilled water (65 °C) for 8 h. The extract was filtered and the solvent was evaporated by using a rotary evaporator, followed by drying in an oven to get powder material. The test solutions (1M HCl) were prepared by diluting analytical grade 37% HCl with distilled water. The CI leaf extract was readily soluble in 1M HCL and test solutions of different concentrations of CI leaf extract ranging from 100 to 750 ppm were prepared and used for mass loss and electrochemical measurements. All tests were carried out without stirring the solutions, under various temperatures.

2.2 Weight Loss Measurement

Weight loss measurements show the inhibition effect of plant extract and provide accurate data of the corrosion process. Rectangular mild steel specimens of 2.5 cm × 2.5 cm × 0.3 cm dimensions were used and experiments were performed at 303 K. These specimens were abraded mechanically using emery papers of different grades, washed with distilled water, degreased, and finally dried. Then the specimens were immersed in the test solution (100 mL) and a solution containing various concentrations of respective inhibitor. All the tests were performed in aerated 1M HCl. All the experiments were conducted in triplicate and average values were noted. Mild steel specimens were removed from test solutions after 10 h, washed with running water, air-dried, before and after corrosion the samples were weighed using an electronic balance (precision ± 0.1 mg).

2.3 Electrochemical Measurements

Electrochemical impedance spectrometry (EIS) and Potentiodynamic polarization (PDP) measurements were carried using Gill Ac instrument under computer control. It is fitted with an assembly of a three-electrode cell consisting of a cylindrical mild steel sample of 1 cm^2 area as the working electrode, platinum as an auxiliary electrode, and saturated calomel electrode as a reference electrode. Before the experimental measurements, three-electrode systems were dipped in 1M HCl solution to get steady-state OCP. EIS measurements were conducted by using AC signals of 10 mV amplitude and the frequency range from 100 kHz to 10 MHz. All EIS data were fitted to equivalent circuits. The Tafel polarization curves were noted by a constant cyclic sweep rate of 60 mV/min from potential − 250 to + 250 mV relative to the E_{corr} value. The studies were conducted at various concentrations from 100 to 750 ppm, at different temperatures and by using oil bath temperature was maintained. Both EIS and PDP measurements were performed subsequently.

2.4 FT-IR Analysis

Fourier Transform Infrared Spectrometer (FTIR) is one of the most effective techniques, which provides accurate information about functional groups present in the form of peaks. Plant extracts contain various organic compounds that are responsible for corrosion inhibition. FTIR spectra were recorded by using IR Prestige-21 Fourier Transform Infrared Spectrometer. FTIR spectra of powdered CI leaf

extract and protective film of CI extract on mild steel in 1M HCl solution was taken out in the wavelength range of 4000–450 cm^{-1}.

2.5 UV-Visible Spectroscopy

Ultraviolet–visible (UV–vis) spectroscopy is performed to determine the adsorption property of inhibitor on mild steel surface in 1M HCl solution with and without CI leaf extract with 10 h of immersion time. UV–vis spectral analysis is carried out using Shimadzu UV-1800 spectrophotometer at a wavelength range of 500–150 nm.

2.6 Scanning Electron Microscopy

The Scanning Electron Microscopy (SEM) is one of the versatile advanced instruments employed for the surface morphology studies. The surface analysis of mild steel specimens before and after immersion in 1M HCl was examined by using FESEM: Sigma series Field Emission Scanning Electron Microscope (Ziess). Pretreated metal coupons were immersed in a 1M HCl solution for 24 h, with and without a CI inhibitor. These specimens were removed from the solution, washed with distilled water, dried, and used for the SEM studies.

3 Results and Discussion

3.1 Weight Loss

Table 1 shows the corrosion behavior of mild steel in 1M HCl in the presence and absence of CI leaf extract at temperature 303 K. The percentage of inhibition efficiency (IE %) was calculated using the following equation [24]

$$IE\% = \frac{W^{\circ} - W}{W^{\circ}} \times 100 \quad (1)$$

where W° and W are the mass loss values without and with inhibitor.

It was observed from Table 1 that, rise in the extract concentration decreases the corrosion rate in 1M HCl and increases the inhibition efficiency of the inhibitor. The decrease in the mild steel weight loss taking place in the 1M HCl solution correlates to an increase in the concentration of CI leaf extract. This suggests that adsorption of phytochemical components of CI leaf extract on mild steel surface by blocking the reaction sites and protect the mild steel metal in a 1M HCl solution. Further, a detailed analysis was carried out using electrochemical techniques to get a better understanding of the corrosion inhibition mechanism of CI leaf extract on mild steel in 1M HCl solution.

Table 1 Weight loss parameters for mild steel in 1M HCl with and without CI leaf extract at 303 K

CI Concentration (ppm)	Weight loss (10^{-3} kg)	IE (%)
Blank	2.3632	
100	0.9022	61.82
250	0.6501	72.49
500	0.5201	77.90
750	0.4112	82.59

3.2 EIS Measurements

Adsorption of inhibitor on the mild steel surface results in a marked increase in impedance of the corrosion system and it causes increased resistance to the charge transfer process. Thus, the potential of an inhibitor can be evaluated by impedance measurements of the corrosion system. It was recorded as a Nyquist plot for mild steel in 1M HCl. Figure 1 shows the Nyquist diagram in 1M HCl for mild steel at various concentrations of inhibitor and temperatures varying from 303 to 323 K. The Nyquist plot appears to be the semicircular shape, but the loops are not the perfect semicircle. This feature can be directly related to surface roughness, electrode irregularity, impurities, adsorption of the inhibitor molecules, and electrode surface inhomogeneity. The diameter of the capacitive loop is increased with increasing concentration of CI leaf extract in acidic medium, due to the localization of CI leaf extract molecules on the active sites of the mild steel surface, leading to the formation of a passive layer on the surface [25, 26].

The Nyquist plots were analyzed in terms of the electrical equivalent circuit with the Zsimpwin 3.20 program. The used electric equivalent circuit consists of R_s (solution resistance) in series with CPE (constant phase element) in parallel to the R_p (polarization resistance), where R_p includes R_{ct} (charge transfer resistance) and R_f (inhibitor film resistance) ($R_p = R_{ct} + R_f$) are represented in Fig. 2. The obtained results from equivalent circuit fitting are shown in Table 2.

The double-layer capacitance (C_{dl}) in the electric equivalent circuit was substituted by CPE, thus avoiding the deviation resulting from the frequency dispersion. C_{dl} and Z_{CPE} can be described as follows [27].

$$Z_{CPE} = Y_0^{-1}(j\omega)^{-n} \quad (2)$$

where Y_0 is the CPE constant, n is the CPE exponent for determining the phase shift that can be used as a measure of surface ruggedness or heterogeneity ($0 \prec n \prec 1$), ω is the angular frequency and $i^2 = -1$ is an imaginary number. However, the double layer capacitances, C_{dl}, were determined for a circuit comprising a CPE by using the following equation [28].

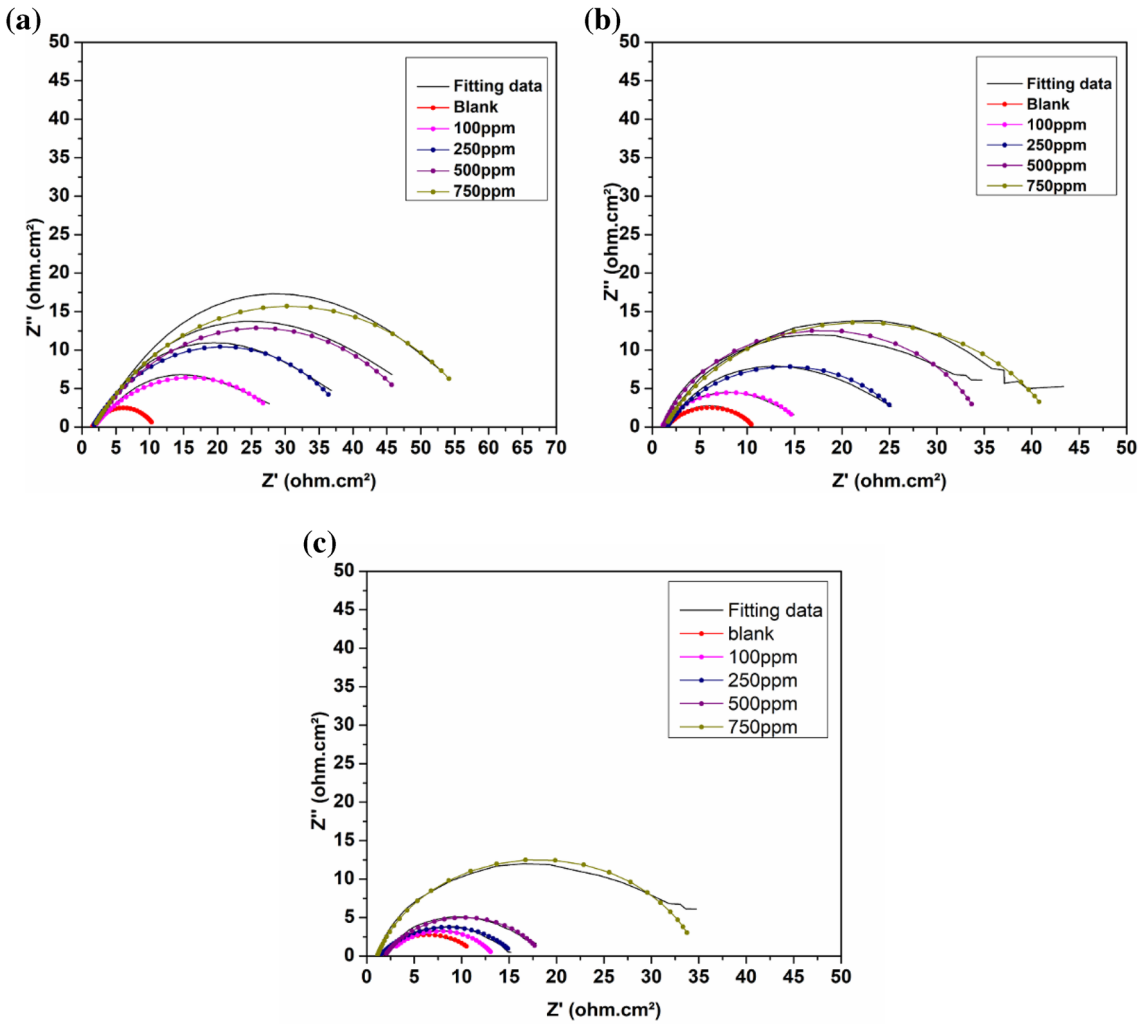

Fig. 1 Experimental and fitted Nyquist diagram in 1M HCl for mild steel at various concentration of CI leaf extract at **a** 303 K, **b** 313 K, and **c** 323 K

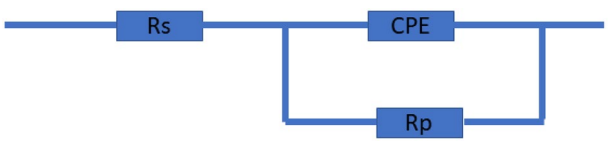

Fig. 2 Equivalent Circuit for EIS data

$$Cdl = \left(Y_0 Rp^{(1-n)}\right)^{1/n} \tag{3}$$

The inhibition efficiency (IE%) was calculated from impedance measurements using the following equation [29].

$$IE\% = \frac{R_p^{\circ} - R_p}{R_p^{\circ}} \times 100 \tag{4}$$

where R_p° and R_p is the polarization resistance in the presence and absence of CI inhibitor. The phytochemical constituents present in the CI leaf extract are adsorbed on the exposed mild steel surface and block the active sites available for corrosive dissolution, increasing the Rp values correlated with inhibitive performance. However, a significant decrease in the C_{dl} with an increase in CI leaf extract was observed due to the decrease in the dielectric constant of the protective layer by replacing the pre-adsorbed water molecules. Decreased dielectric constant strengthens the adsorption capability of CI leaf extract [30, 31]. This can be explained by better coverage and protection of the mild steel metal against dissolution, as confirmed by the increase in inhibition performance with the concentration of the CI leaf extract as shown in Table 2

Bode plots for mild steel in an acidic environment at varying temperatures (303–323 K) are represented in Fig. 3. It is evident from the literature that, ideal phase angle and slope value should be -90^0 and -1 respectively. In the present study, deviation takes place from the ideal capacitive behavior,

Table 2 EIS parameters for mild steel in 1M HCL in the absence and presence of CI leaf extract at 303 K, 313 K, and 323 K

Temperature (K)	Concentration (ppm)	R_s (Ω·cm^2)	CPE Y_0 (μS cm^{-2}S^{n2})	n	R_p (Ω·cm^2)	C_{dl} (μF·cm^{-2})	IE (%)
303	Blank	1.517 (1.6%)	316 (9.5%)	0.62 (2.1%)	9.22 (2.3%)	362	
	100	1.769 (3.6%)	180 (8.8%)	0.54 (2.0%)	28.47 (2.9%)	143	67.61
	250	1.576 (2.9%)	89 (8.1%)	0.63 (1.6%)	38.30 (2.7%)	122	75.90
	500	1.743 (4.9%)	77 (9.8%)	0.61 (2.0%)	48.83 (3.3%)	94.5	81.11
	750	1.777 (4.5%)	58 (9.6%)	0.63 (1.9%)	57.59 (3.3%)	78.8	83.99
313	Blank	1.508 (2.6%)	151 (8.7%)	0.64 (1.8%)	9.17 (1.5%)	136	
	100	0.995 (2.4%)	123 (7.2%)	0.69 (1.3%)	14.77 (2.0%)	203	37.9
	250	1.569 (2.2%)	106 (8.5%)	0.70 (1.6%)	25.30 (2.7%)	225	63.75
	500	1.138 (2.4%)	41 (8.7%)	0.81 (1.4%)	33.71 (2.7%)	151	72.79
	750	1.418 (2.0%)	37 (6.4%)	0.74 (1.0%)	41.02 (1.9%)	87.1	77.64
323	Blank	1.439 (1.8%)	395 (8.8%)	0.63 (2.0%)	10.18 (2.7%)	598	
	100	1.856 (1.9%)	320 (8.2%)	0.69 (1.9%)	12.70 (2.2%)	759	19.8
	250	1.374 (1.7%)	361 (6.8%)	0.61 (1.6%)	14.29 (1.9%)	542	28.76
	500	1.902 (2.6%)	118 (9.7%)	0.68 (1.9%)	16.67 (2.3%)	186	38.93
	750	1.160 (3.4%)	96 (9.1%)	0.65 (1.8%)	38.87 (2.7%)	163	73.81

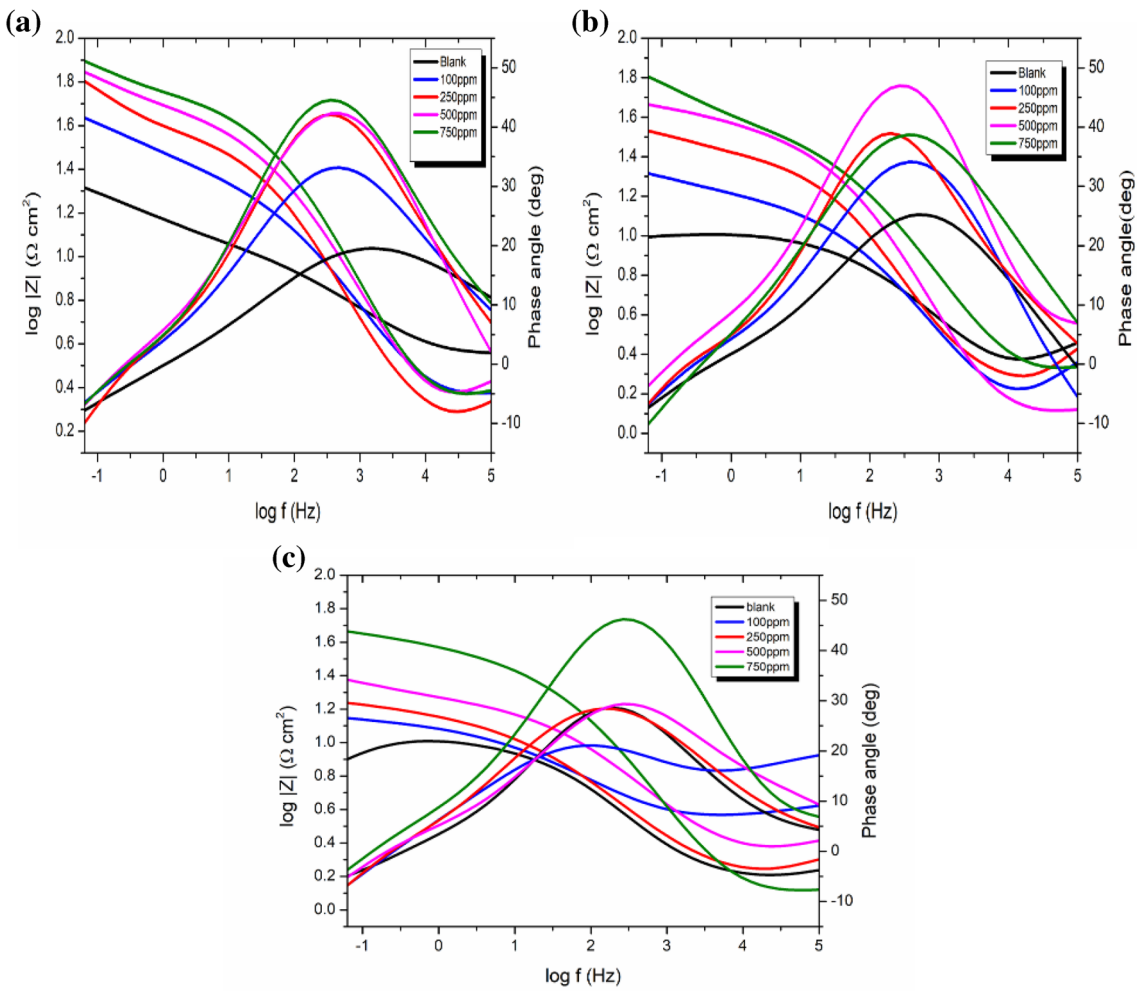

Fig. 3 The Bode plot in 1M HCl for mild steel at various concentrations of CI leaf extract at **a** 303 K, **b** 313 K, and **c** 323 K

this is due to the rough surface of metal (mild steel) electrodes. The roughness on the mild steel surface in the acidic medium occurs due to the accumulation of corrosion products [32, 33]. From Bode plots, it is shown that the phase angle is gradually increased in the presence of CI inhibitor, indicating that the metal (mild steel) surfaces were less corroded and the inhibitors formed a protective film in acidic solution on the mild steel surface and protected against acid corrosion. The result of the EIS technique employed is in good agreement with the weight loss technique.

3.3 Potentiodynamic Polarization Measurements

Further to understand the mechanism of the CI leaf extract studied, measurements of the polarization curve for mild steel were also tested in an acidic environment. Potentiodynamic polarization plots showing the effect of CI on an anodic and cathodic process in 1M HCl for mild steel at all tested temperatures were shown in Fig. 4.

The extrapolation of the Tafel plots allows the calculation of electrochemical polarization parameters such as i_{corr} (corrosion current density), E_{corr} (corrosion potential), βa (anodic Tafel slope), and βc (cathodic Tafel slope). The values of electrochemical polarization parameters and IE% are given in Table 3. The inhibition efficiency (η%) and surface area coverage (θ) were calculated using the following equations. [34].

$$\eta\% = \frac{i^{o}_{corr} - i_{corr}}{i^{o}_{corr}} \times 100 \tag{5}$$

$$\theta = 1 - \frac{i_{corr}}{i^{o}_{corr}} \tag{6}$$

where i^{0}_{corr} and i_{corr} represent corrosion current density values in the uninhibited and inhibited mild steel specimen. The results shown in Table 3 indicate that the adsorption of CI leaf extracts altered the mechanism of anodic dissolution and cathodic hydrogen evolution. Inhibitive ability, which is denoted by η % is remarkably increased with the addition of CI leaf extract. It suggests that there is an adsorption of CI leaf extract molecules and the formation of a protective film on the surface of mild steel [35]. In addition to the

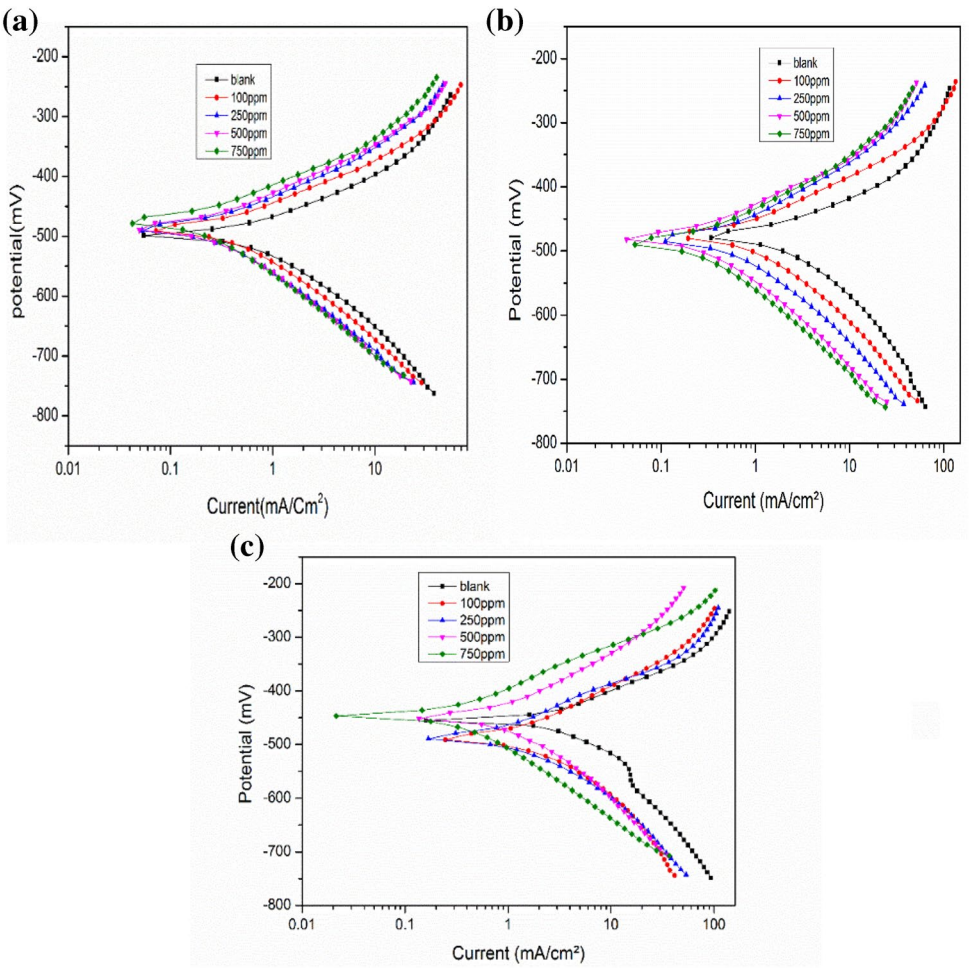

Fig. 4 Polarization curves for mild steel in 1M HCl solution without and with various concentrations of CI leaf extract at **a** 303 K, **b** 313 K, and **c** 323 K

Table 3 Potentiodynamic polarization parameters for mild steel in 1M hydrochloric acid containing different concentrations of CI Leaf extract at 303 K, 313 K, and 323 K

Temperature (K)	C (ppm)	i_{corr} (mA/cm^2)	E_{corr} (mV/SCE)	βa (mV)	βc (mV)	Corrosion rate(mm/year)	(η %)	Θ
303	blank	1.3425	– 497.2	112.6	178.65	15.56		
	100	0.5031	– 485.71	88.63	137.95	05.83	62.52	0.6252
	250	0.3718	– 485.6	98.45	133.67	04.30	70.76	0.7076
	500	0.3142	– 483.97	92.44	137.51	03.64	76.55	0.7655
	750	0.2761	– 476.24	92.41	133.73	03.20	79.48	0.7948
313	blank	2.0668	– 475.27	88.61	107.20	23.95		
	100	1.1528	– 475.27	99.25	102.83	13.36	44.22	0.4422
	250	0.7288	– 479.77	171.53	161.52	08.44	64.73	0.6473
	500	0.5081	– 444.25	94.81	141.94	05.88	75.41	0.7541
	750	0.4751	– 484.59	102.96	153.96	05.50	77.01	0.7701
323	blank	2.2555	– 450.83	85.55	93.893	26.14		
	100	1.8790	– 487.55	110.08	164.68	21.77	16.67	0.1667
	250	1.4940	– 485.78	113.74	192.73	17.31	33.74	0.3374
	500	1.3434	– 446.87	136.51	164.96	15.57	40.44	0.4044
	750	0.5822	– 444.25	100.47	140.60	06.74	74.19	0.7419

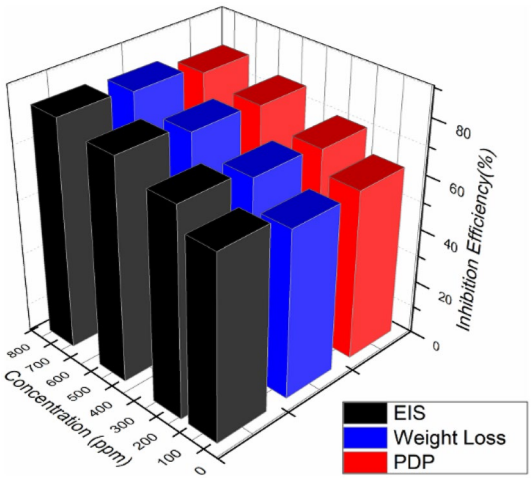

Fig. 5 Inhibition Efficiency of CI leaf extract obtained from different techniques

results, it is found from the literature that if E_{corr} is greater than ± 85 mV / SCE compared to the blank acid solution, the inhibitor may be classified as a cathodic or anodic type whereas, if the E_{corr} value is less than ± 85 mV / SCE, the inhibitor may be classified as a mixed type [36]. In the present work, the E_{corr} value is minutely displaced in the presence of an inhibitor. Therefore, CI leaf extract is proved to be a mixed type of inhibitor.

On the other hand, the data obtained from PDP methods are in excellent accordance with those results obtained from gravimetric and EIS methods. Figure 5 represents the inhibition efficiency obtained from various methods and reveals that EIS measures were higher than those obtained from other techniques.

3.4 Effect of Temperatures

Temperature is an important parameter as it allows for evaluation of the nature of inhibitor adsorption on the metal surface and the impact of temperature on the inhibitor's ability. The corrosion inhibition performances of the CI inhibitor were further investigated for mild steel in 1M HCl at a temperature ranging from 303 to 323 K by electrochemical measurements. According to Fig. 1, it is seen that the diameter of the capacitive loop of the Nyquist plot is decreased significantly with an increase in temperature for mild steel in 1M HCl. It is clear from Table 2, that the Rp values and the inhibition efficiency of CI leaf extract decreased markedly with a rise in the temperature, reaching minimum efficiency at 323 K. The decrease in IE% may be due to the desorption of inhibitor molecules from the metal surface and temperature reduces the ability of CI inhibitor molecule to adsorb on the mild steel surface at an elevated temperature.[37]. As shown in Fig. 4 the Tafel curve moves towards the direction of high current with an increase in temperature from 303 to 323 K. This indicates that the effect of the inhibitor on mild steel decreases as the temperature rises. Inspection of the data from Table 3 shows that the corrosion rate (CR) of mild steel and i_{corr} values in aggressive solutions increase with a rise in temperature. This is due to a reduction in the hydrogen evolution overpotential, which results in higher metal dissolution rates [38]. It was found that the inhibitory efficiency decreases with a rise in temperature, according

to the results obtained from the temperature effect for both the EIS and PDP methods. These results show that the corrosion inhibition efficiency of CI leaf extract is not well at the higher temperature. It is genuinely a serious issue which will restrict the extract's practical application. The strategy to enhance the efficiency of plant extracts inhibition performance at higher temperatures will be further explored in future research. In acidic solution, the effect of temperature on the corrosion rate of mild steel was related to temperature by following the Arrhenius equation [39]

$$\text{LogCR} = \frac{-\text{Ea}}{2.303\text{RT}} + \log \text{A} \tag{7}$$

where Ea is the activation energy, R is the universal gas constant (8.314 J K^{-1} mol^{-1}), T is the absolute temperature (K) and A is the Arrhenius factor. Figure 6 shows the plot of Log CR vs 1/T for mild steel in 1M HCl solution at different concentrations of inhibitors. Where the slope is (-Ea/2.303R) and intercept is log A. The slopes values have been observed and Ea values were calculated.

Table 4 illustrates the calculated Ea values. The activation energy for the system containing CI leaf extract in 1M HCl was higher than the blank solution. In the presence of CI leaf extract, the greater activation energy value shows that the slow corrosion process and sensitivity to temperature changes. An increase in Ea in the presence of a CI leaf extract inhibitor indicates the physisorption process [40]. The kinetic parameters like enthalpy ($\Delta H^{0}_{a)}$ and entropy (ΔS^{o}_{a}) of the corrosion process in acidic medium was calculated using the following transition state equation [41].

$$CR = \frac{RT}{Nh} \exp\left(\frac{\Delta S^{\circ}_{a}}{R}\right) \exp\left(\frac{-\Delta H^{\circ}_{a}}{RT}\right) \tag{8}$$

Table 4 Activation parameters for mild steel in 1M HCl

C (ppm)	Ea (kJ mol^{-1})	ΔH°_{a} (kJmol^{-1})	ΔS°_{a} (J mol^{-1} K^{-1})
Blank	20.74	18.21	− 161.73
100	52.34	49.81	− 65.66
250	55.00	52.54	− 59.69
500	57.17	54.66	− 54.68
750	29.72	27.15	− 145.39

where N is Avogadro's number, h is Planck's constant. R is the gas constant, ΔH°_{a} and ΔS°_{a} are respectively the enthalpy and entropy of activation. A plot of $\text{Log}\left(\frac{\text{CR}}{\text{T}}\right)$ vs 1/T provides straight lines with a slope of $\frac{-\Delta H^{\circ}_{a}}{2.303\text{R}}$ and an intercept of $\text{Log(R/Nh)} + \Delta S^{o}_{a}/2.303\text{R}$ is represented in Fig. 7.

Calculated values of enthalpy and entropy are illustrated in Table 4. The positive value of ΔH°_{a} in the presence of CI leaf extract indicates the endothermic nature of the process of metal dissolution, suggesting the physisorption process. Large negative values of ΔS°_{a} imply the activated complex in the rate-determining step, represents an association step rather than a dissociation step, which indicates that an increase in the orderliness in the activated complex. This behavior is mainly due to the replacement of water molecules by the adsorption of inhibitor molecules on mild steel [42, 43].

3.5 Fourier-Transform Infrared Spectroscopy (FTIR)

The presence of organic molecules in the extract may assist the adsorption of inhibitor on a mild steel surface to reduce corrosion. In the current work, Fig. 8 represents the FTIR spectrum of CI leaf extract and that of the protective film formed on the mild steel surface when the CI leaf extract was

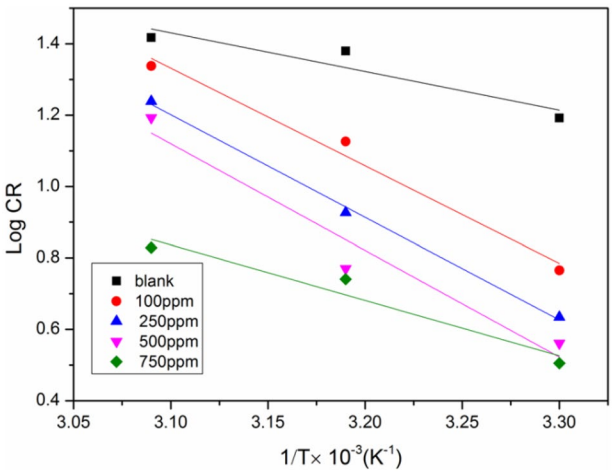

Fig. 6 Arrhenius plot for mild steel corrosion in 1M HCl

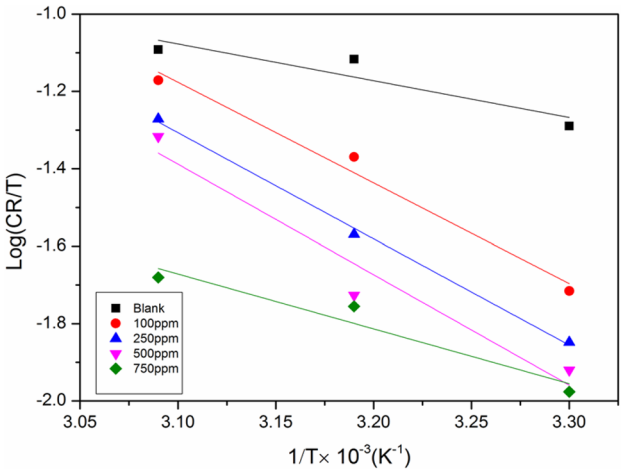

Fig. 7 The plot of Log (CR/T) vs 1/T in 1.0 M HCl at different concentration of inhibitors system

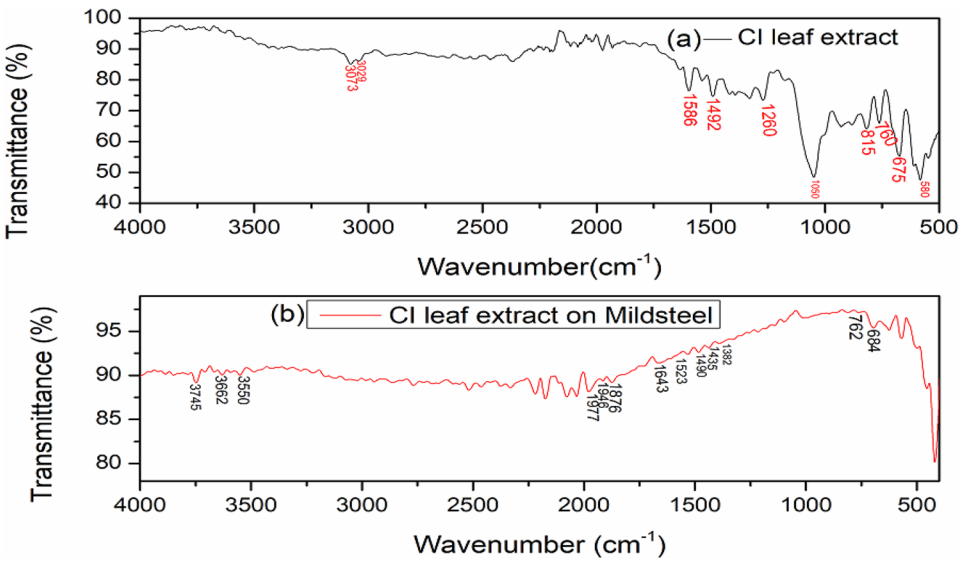

Fig. 8 FT-IR spectra of (a) CI leaf extract and (b) CI leaf extract on mild steel

used as an inhibitor. From Fig. 8a, it was found that a peak of 3073 cm^{-1} and 3029 cm^{-1} were attributed to the C–H aromatic stretching. The presence of functional group N–O was confirmed from peaks 1586 cm^{-1} and 1492 cm^{-1}. The peak 1260 cm^{-1} has assigned to C–O stretching. 1050 cm^{-1} corresponds to C–O (ether) stretching. C–H bend was noted at 815 cm^{-1} and 760 cm^{-1}. Peaks at 675 cm^{-1} and 580 cm^{-1} corresponds to C–I stretching. Further, from Fig. 8b it was found that N–O stretch at 1586 cm^{-1} and 1492 cm^{-1} was shifted to 1523 cm^{-1} and 1490 cm^{-1}, this variation in the frequency values indicating the interaction between the CI leaf extract and mild steel surface. Other bands at 450–800 cm^{-1} possibly originates from corrosion product Fe_2O_3 (684 cm^{-1}). Many functional groups in the protective film were missing indicating that the inhibitor adsorption on the surface of mild steel may have occurred through the missing bonds. The results from FTIR shows that the inhibitive efficiency of CI leaf extract is mainly due to the presence of functional groups which exist in the extract and involved in the formation of bond with Fe in mild steel in 1M HCl and that makes the CI leaf extract desirable for corrosion inhibition purposes.

3.6 UV–Visible Spectroscopy

The UV spectra of CI leaf extract with 1M HCl prior and then afterward 10 h of immersion of mild steel specimens were recorded and are shown in Fig. 9. The electronic absorption spectra of CI leaf extract without a mild steel sample show peaks of higher absorbance in the UV region. These peaks get shifted after the immersion of mild steel samples. The shift in the absorbance value indicates the adsorption of CI inhibitor molecules from the solution on the metal surface [44]. Based on this fact, it may be inferred

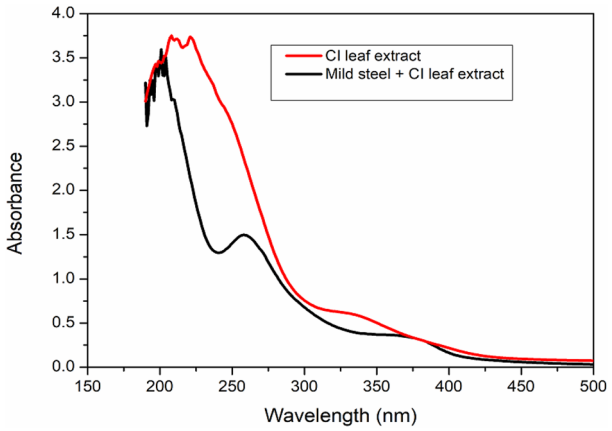

Fig. 9 UV Spectra of CI leaf extract before and after immersion of mild steel sample

that the phytochemical components are present in the CI leaf extract have been adsorbed on the surface of mild steel and prevents corrosion.

3.7 Scanning Electron Microscopy (SEM)

The surface morphology was used to show the inhibition of corrosion due to the formation of a protective layer on the metal surface. Figure 10 depicts the micrographs of mild steel samples 1M HCl, in the absence and presence of CI leaf extract after 24-h immersion. Figure 10a represents the uninhibited mild steel surface which was strongly damaged and showed the disappearance of the metal surface due to an aggressive acidic environment. Figure 10b indicates a fairly smoother surface, by the addition of CI leaf extract to the test solution. This could be

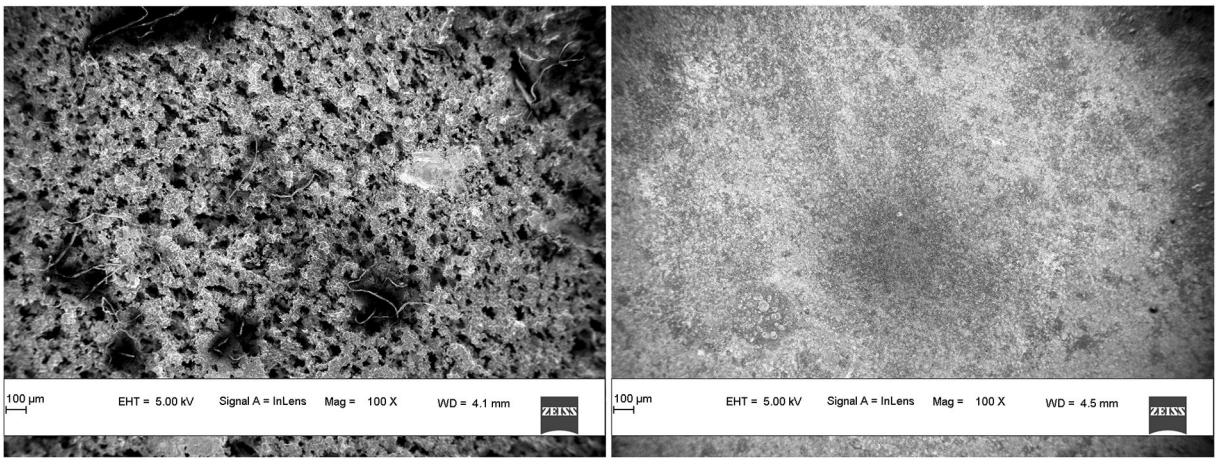

Fig. 10 Surface morphology of mild steel before and after immersion for 24 h in 1M HCl without and with inhibitor

due to the adsorption of organic molecules present in the plant extract. These findings proved that the leaf extract of CI has created a protective film and can efficiently reduce steel surface corrosion.

3.8 Inhibition Mechanism

In general, CI leaf extract contains amino acids, carbohydrates, alkaloids, protein, tannins, the hetero atoms like S, N, O, etc., that can serve as a reaction centres for the adsorption process. The effective molecules of CI leaf extracts are water-soluble. The inhibition process involves the formation of a protective layer on the metal surface by replacement of the water molecules adsorbed on the surface of the metal with inhibitor molecules.

$$(\text{Inhibitor})_{\text{sol}} + \left(\text{nH}_2\text{O}\right)_{\text{ads on metal surface}} \leftrightarrow \left(\text{nH}_2\text{O}\right)_{\text{sol}} + (\text{Inhibitor})_{\text{ads on metal surface}}.$$

Adsorption of inhibitor molecule onto metal surface takes place though physisorption or chemisorption. The corrosion inhibition efficiency depends on the number of adsorption sites, molecular size, and mode of interaction with metal stability and charge density. In the present study, CI leaf extract contains many phytochemical constituents, hence it was unable to specify a particular compound and explain the inhibition mechanism. Figure 11 represents the general inhibition mechanism. From the results obtained by electrochemical and gravimetric

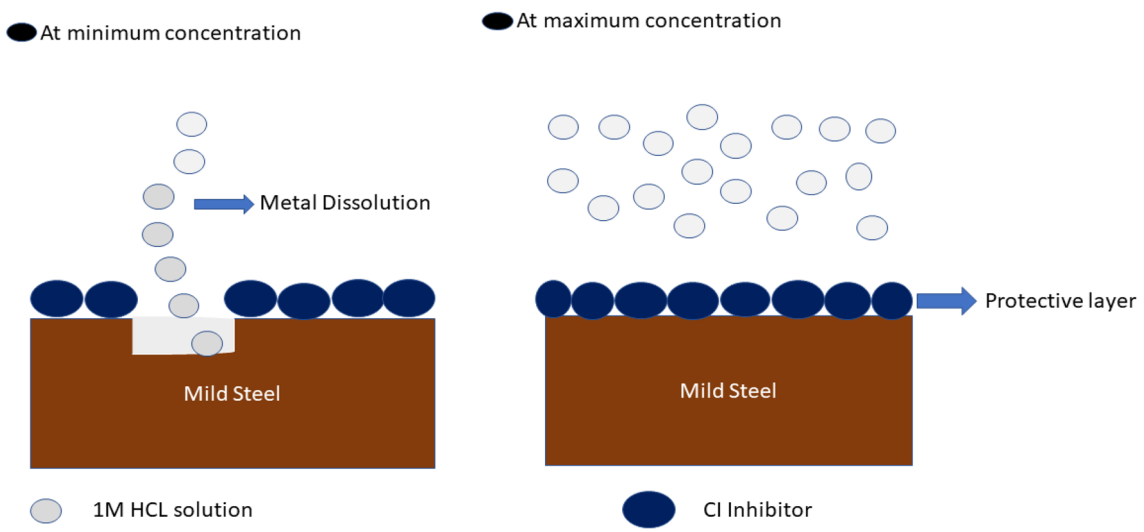

Fig. 11 Schematic representation of adsorption CI inhibitor molecules on mild steel surface in 1M HCl solution

measurements, it can be ascertained that the CI extract acts as an effective inhibitor due to a higher tendency of CI extract molecules to adsorb on mild steel in the 1M HCl solution. From the kinetic studies and thermodynamic analysis, it is observed that adsorption of CI leaf extract on mild steel surface involves the physical adsorption process. Hence CI molecules are more effectively adsorbed over metal surface and act as an efficient eco-friendly inhibitor.

3.9 Comparison of Inhibition Efficiency

Corrosion inhibition activity of *Allium sativum* [45] extract has been investigated for mild steel and the maximum efficiency was found to be 76.47% in 1M HCl. *Sweet potato tuber* (*PMS)* [46] extract, obtained with solvent n-hexane has been reported to effectively inhibit the corrosion of mild steel in 1M HCl and the maximum efficiency of 64.26% was obtained at a maximum concentration of 0.7 g/L. Furthermore, *Dioscorea septemloba* [47] extracts with 2 g/L concentration also showed 72.1% inhibition efficiency according to the EIS tests on carbon steel in 1M HCl. In this work, aqueous CI leaf extract showed better inhibition from the literature value. The corrosion inhibition performance of CI leaf extract on mild steel at 303 K was up to 83.99% at 750 ppm concentration. Hence aqueous CI leaf extract proved to be a novel eco-friendly and low-cost green inhibitor due to its simple extraction method and good inhibition efficiency for mild steel in 1M HCL.

4 Conclusion

Combretum Indicum (CI) leaf extract showed good inhibition of corrosion in 1M HCl. The inhibition efficiency of CI leaf extract improved with higher concentration and reduced with higher temperatures. It reveals that inhibition effectiveness depends on temperature and concentration of inhibitor. Polarization trials have shown that the CI leaf extract is a mixed type inhibitor. Calculation of activation parameters indicates the strong interaction between inhibitor molecules and the surface of the mild steel. SEM micrographs for medium containing inhibitor showed the smoother surface in 1M HCl solution and its inhibition by CI leaf extract.

Acknowledgements Authors gratefully acknowledge the support of Dr. Arun M Isloor and Dr. A Nityananda Shetty of National Institute of Technology Karnataka for providing instrumental facility to carry out electrochemical studies

Compliance with ethical standards

Conflict of Interest The Corresponding author states that there is no conflict of interest.

References

1. Vu NSH, Binh PMQ, Dao VA, Thu VTH, Van Hien P, Panaitescu C, Nam ND (2020) J Mol Liq. https://doi.org/10.1016/j.molliq.2020.113787
2. Ikhmal WMKWM, Maria MFM, Rafizah WAW, Norsani WNWM, Sabri MM (2019) Int J Corros Scale Inhib 8:628–643
3. Fouda AS, Eissa M, Fakih M (2019) J Bio- Tribo-Corros 5:5–17
4. Faiz M, Zahari A, Awang K, Hussin H (2020) RSC Adv 10:6547–6562
5. Sedik A, Lerari D, Salci A, Athmani S, Bachari K, Gecibesler İH, Solmaz R (2020) J Taiwan Inst Chem Eng 107:189–200
6. Sanaei Z, Ramezanzadeh M, Bahlakeh G, Ramezanzadeh B (2019) J Ind Eng Chem 69:18–31
7. Dehghani A, Bahlakeh G, Ramezanzadeh B, Ramezanzadeh M (2020) J Mol Liq. https://doi.org/10.1016/j.molliq.2019.112046
8. Jayakumar S, Nandakumar T, Vadivel M, Thinaharan C, George RP, Philip J (2020) J Adhes Sci Technol 34:713–743
9. Ferdosi Heragh M, Tavakoli H (2019) Met Mater Int. https://doi.org/10.1007/s12540-019-00453-6
10. Alibakhshi E, Ramezanzadeh M, Bahlakeh G, Ramezanzadeh B, Mahdavian M, Motamedi M (2018) J Mol Liq 255:185–198
11. Qiang Y, Zhang S (2018) TanB, Chen S. Corros Sci 133:6–16
12. Baran E, Cakir A, Yazici B (2019) Arab J Chem 12:4303–4319
13. Mbah CN, Onah CC, Nnakwo KC (2020) Eng Res Express 2:015039–015051
14. Akinbulumo OA, Odejobi OJ, Odekanle EL (2020) Results Mater 5:100074–100080
15. Okewale AO, Adesina OA (2020) J Appl Sci Environ Manag 24:37–47
16. Bhuvaneswari TK, Jeyaprabha C, Arulmathi P (2020) J Adhes Sci Technol. https://doi.org/10.1080/01694243.2020.1766395
17. Bhardwaj N, Prasad D, Haldhar R (2018) J Bio- Tribo-Corros 4:61–70
18. Li D, Zhang P, Guo X, Zhao X, Xu Y (2019) RSC Adv 9:40997–41009
19. Haldhar R, Prasad D, Saxena A (2018) J Environ Chem Eng 6:5230–5238
20. Boumhara K, Harhar H, Tabyaoui M, Bellaouchou A, Guenbour A, Zarrouk A (2019) J Bio- Tribo-Corros 5:8–16
21. Ezeamaku UL, Iheaturu NC, Chike KO, Onukwuli OD (2019) Int J Adv Res Chem Sci 6:1–9
22. Vasanthajothi R, Saratha R, Krishnaveni K (2020) J Adhes Sci Technol. https://doi.org/10.1080/01694243.2020.1801248
23. Bhuiya NMA (2020) Int J Green Pharm (IJGP) 14:169–174
24. Anupama KK, Joseph A (2018) J Bio- Tribo-Corros 4:30–43
25. Fernandes CM, Fagundes TDSF, dos Santos NE, Rocha TSDM, Garrett R, Borges RM, Muricy G, Valverde AL, Ponzio EA (2019) Electrochim Acta 312:137–148
26. Boudjellal F, Ouici HB, Guendouzi A, Benali O, Sehmi A (2020) J Mol Struct 1199:127051–127063
27. Singh A, Ansari KR, Chauhan DS, Quraishi MA, Lgaz H, Chung IM (2020) J Colloid Interface Sci 560:225–236
28. Rbaa M, Lgaz H, El Kacimi Y, Lakhrissi B, Bentiss F, Zarrouk A (2018) Mater Discov 12:43–54
29. Berrissoul A, Ouarhach A, Benhiba F, Romane A, Zarrouk A, Guenbour A, Dikici B, Dafali A (2020) J Mol Liq 313:113493–113508
30. Dehghani A, Bahlakeh G, Ramezanzadeh B, Ramezanzadeh M (2019) J Mol Liq 277:895–911
31. Chaouiki A, Chafiq M, Lgaz H, Al-Hadeethi MR, Ali IH, Masroor S, Chung IM (2020) Coatings 10:640–656
32. Dohare P, Quraishi MA, Obot IB (2018) J Chem Sci 130:8–26
33. Haldhar R, Prasad D, Saxena A, Kumar R (2018) Sustain Chem Pharm 9:95–105

34. Bhuvaneswari TK, Vasantha VS, Jeyaprabha C (2018) Silicon 10:1793–1807
35. Khattabi M, Benhiba F, Tabti S, Djedouani A, El Assyry A, Touzani R, Warad I, Oudda H, Zarrouk A (2019) J Mol Struct 1196:231–244
36. Saxena A, Prasad D, Haldhar R, Singh G, Kumar A (2018) J Environ Chem Eng 6:694–700
37. Thomas A, Prajila M, Shainy KM, Joseph A (2020) J Mol Liq 312:113369–113381
38. Bahlakeh G, Dehghani A, Ramezanzadeh B, Ramezanzadeh M (2019) J Mol Liq 293:111559–111574
39. Haque J, Ansari KR, Srivastava V, Quraishi MA, Obot IB (2017) J Ind Eng Chem 49:176–188
40. Fouda AEAS, Shahba RMA, El-Shenawy AE, Seyam TJA (2018) Int J Electrochem Sci 13:7057–7075
41. Barrahi M, Elhartiti H, El Mostaphi A, Chahboun N, Saadouni M, Salghi R, Zarrouk A, Ouhssine M (2019) Int J Corros Scale Inhib 8:937–953
42. Mobin M, Aslam R, Aslam J (2017) Mater Chem Phys 191:151–167
43. Ahmed SK, Ali WB, Khadom AA (2019) Int J Ind Chem 10:159–173
44. Saxena A, Prasad D, Haldhar R (2018) J Mater Sci 53:8523–8535
45. Ojha LK, Tüzün B, Bhawsar J (2020) J Bio- Tribo-Corros 6:1–10
46. Anyiam CK, Ogbobe O, Oguzie EE, Madufor IC, Nwanonenyi SC, Onuegbu GC, Obasi HC, Chidiebere MA (2020) SN Appl Sci 2:520–530
47. Emori W, Zhang RH, Okafor PC, Zheng XW, He T, Wei K, Lin XZ, Cheng CR (2020) Colloids Surf, A 590:124534–124546